NUCLEAR INSTRUMENTS AND METHODS 149 (1978) 271-277 ; © NORTH-HOLLAND PUBLISHING CO.

Part IV. Analysis by nuclear reactions

THE USE OF ^{6}Li AND ^{35}Cl ION BEAMS IN SURFACE ANALYSIS

J. L'ECUYER, C. BRASSARD, C. CARDINAL

Laboratoire de Physique Nucléaire, Université de Montréal, C.P. 6128, Montréal H3C 3T4, Québec, Canada

and

B. TERREAULT

Centre de l'Energie, INRS, Université de Québec, C. P. 1020 Varennes J0L 2PO, Québec, Canada

1. Introduction

The detection of light elements in materials presents many difficulties, and some standard techniques (e.g., Rutherford backscattering) are difficult or impractical. The present paper reviews attempts that have been made to find general and reliable methods of profiling light elements in a way similar to the Rutherford backscattering spectrometry.

Nuclear reactions have been used for many years to detect and profile many of the light elements[1]). In general, a specific beam such as a proton beam has been used to detect a particular isotope like ^{18}O through a particular reaction, here ^{18}O(p, α)^{15}N. The same beam can sometimes be used to detect other elements. One approach to the problem of finding a general method of light elements detection would be to find an ion beam capable of inducing, in most light nuclei, nuclear reactions suitable for analysis.

In order to be of analytic interest, methods of this type must meet the following general criteria: (1) good selectivity, i.e., an easily recognizable spectrum with a few well separated levels showing up in a relatively background-free region; (2) good depth resolution; (3) reasonable cross section.

We will now discuss two techniques which generally meet these criteria: (a) ^{6}Li-induced nuclear reactions[2]) and (b) detection of light nuclei recoiling after being hit by a heavy incoming ion[3]).

2. ^{6}Li-induced nuclear reactions

^{6}Li is a weakly bound nucleus. This characteristic explains why all (^{6}Li, p), (^{6}Li, d), and (^{6}Li, α) reactions on nuclei between Li and Ne have positive Q values, generally above 10 MeV for (^{6}Li, p)

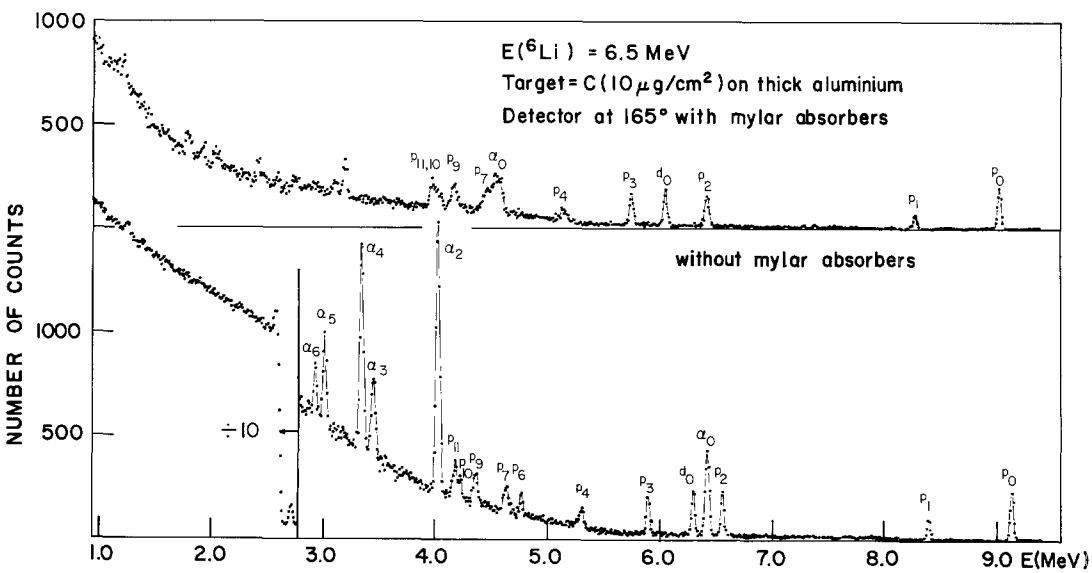

Fig. 1. Particle spectra from the ^{6}Li bombardment of a 45 nm carbon layer on a thick aluminium backing. The top spectrum was obtained with a 19 μm mylar absorber in front of the detector; and the bottom spectrum, without absorber. The numbers refer to the energy levels of the residual nuclei. The RBS spectrum of ^{6}Li can be observed at low energy in the bottom spectrum.

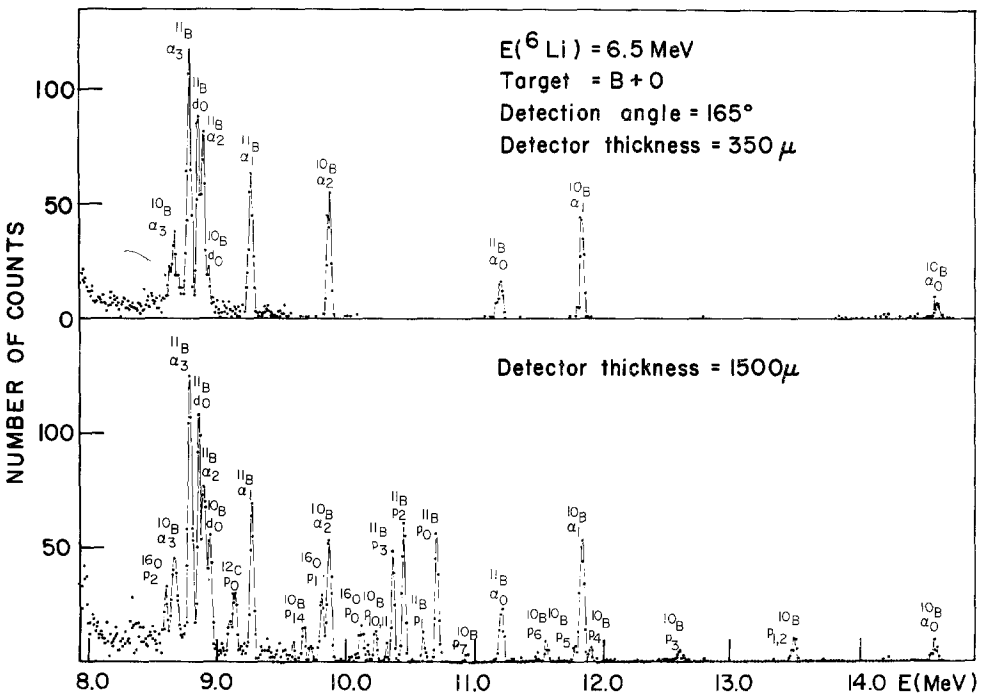

Fig. 2. Particle spectra from the bombardment of a natural boron target. Since it had been exposed to air for a considerable time, oxygen and carbon are clearly seen. The top spectrum was taken with a 350 μm detector which did not stop protons of energy exceeding 7 MeV or deuterons above 9 MeV.

and (^{6}Li, α). This property is the main reason to choose a ^{6}Li beam for analytical purposes.

2.1. Selectivity

The high Q value ensures that the reaction products of interest will generally have a higher energy than the scattered ^{6}Li beam (fig. 1). The reaction products together with the backscattering spectrum can sometimes be observed without an absorber. Even if it is necessary to use an absorber to stop the high flux of scattered ^{6}Li ions, the higher energy protons, deuterons, and alphas will easily go through; and their resolution will not be greatly deteriorated. Fig. 1 also shows that at 6.5 MeV, an aluminium matrix does not contribute to the reaction products. Since this is only 3 MeV below the Coulomb barrier for ^{6}Li on Al, one can appreciate the rapid drop in cross section below the Coulomb barrier.

In cases where many light nuclei are present, it is sometimes necessary to distinguish among the various reaction products. This can be done by varying the detector thickness so that protons or deuterons lose only part of their energy in the sensitive region of the detector (fig. 2). Other more sophisticated devices such as a ΔE–E counter telescope can also be used[4]) to identify precisely the type of reaction products.

2.2. Depth resolution

The depth resolution is best characterised by the depth factor defined as

$$F = \frac{k}{\cos\theta_1}\left(\frac{dE}{dx}\right)_1 + \frac{1}{\cos\theta_2}\left(\frac{dE}{dx}\right)_2 \quad \text{(see fig. 3)},$$

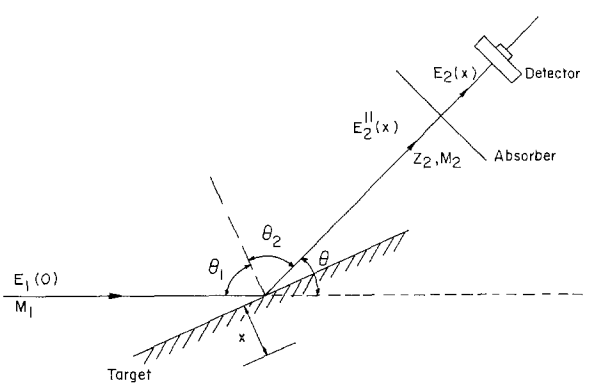

Fig. 3. Experimental setup in the reflexion geometry. $E_2''(x)$ is the energy of the outgoing particle on leaving the target; and $E_2(x)$, its energy when reaching the detector. In the absence of an absorber, $E_2''(x) = E_2(x)$.

TABLE 1

Depth factor F and depth resolution without (Δ_N) and with (Δ_A) absorber for various reactions used in the detection of ^{16}O in copper at beam energy E_1 (0). $F^{(1)}$ and $\Delta^{(1)}$ are calculated for a detection angle $\theta = 165°$ and a target tilt angle $\theta_1 = 0°$. $F^{(2)}$ and $\Delta^{(2)}$ are for $\theta = 40°$ and $\theta_1 = 65°$.

Reaction	E_1 (0) (MeV)	$F^{(1)}$ (MeV·cm^2/mg)	$F^{(2)}$ (MeV·cm^2/mg)	$\Delta_N^{(1)}$ (nm)	$\Delta_A^{(1)}$ (nm)	$\Delta_A^{(2)}$ (nm)
d, p	1.0	0.19	0.65	118	206	60
α, α	4.0	0.90	–	25	–	–
^{6}Li, p	6.0	0.59	2.39	38	66	16
^{6}Li, α	6.0	0.73	3.46	30	95	20
^{6}Li, ^{6}Li	6.0	1.63	–	20	–	–

where $(dE/dx)_1$ and $(dE/dx)_2$ are the mean specific energy loss of the incoming and outgoing particles[5]). The kinematic factor is here an approximation implying a linear relationship $E_2 = kE_1 + E'$ between the energy of the particles just before and after the reaction. It is generally valid, over the limited energy range under consideration. With this approximation the outgoing particle energy is given by

$$E_2(x) = kE_1(0) + E' - Fx.$$

Table 1 shows the depth factor F of various reactions used for detecting ^{16}O in copper at 165°, with the estimated depth resolution if a mylar absorber is used to stop the elastically scattered ions. The stopping-power tables of Northcliffe and Schilling were used to obtain values of dE/dx [6]).

Because ^{6}Li-induced reactions are usually highly exothermic, it is good to work at forward angles where the kinematic factor is larger. In table 1 we have indicated the value of 40°. Depth resolutions of a few hundred Ångstroms can be obtained in this manner.

The maximum depth that can be explored depends on the spacing between the energy levels and on the rapid drop in cross section as the energy of the ^{6}Li particle decreases below the Coulomb barrier. In general the maximum depth is about a few micrometers. For instance, in fig. 4 the energy difference between p_1 and p_2 is 0.41 MeV. With a depth factor of 0.11 MeV/μm, this energy difference

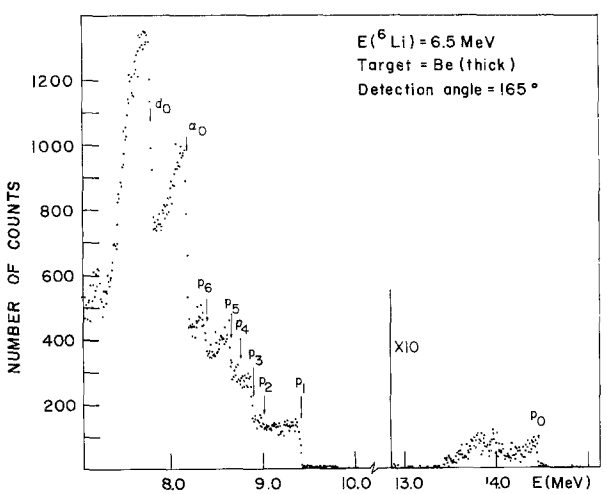

Fig. 4. Particle spectrum from the bombardment of a thick Be target. The arrows represent the calculated energy of the particles coming from the surface. The width of the p_0 peak is approximately 1 MeV, corresponding to a probing depth of 9 μm. With the p_1 peak, 3.7 μm can be explored.

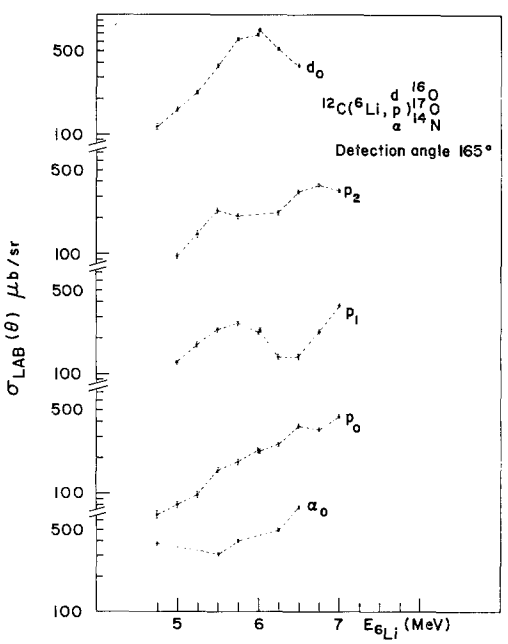

Fig. 5. Excitation function (lab) of the reaction ^{12}C(^{6}Li, x) at 165°.

corresponds to a thickness of 3.7 μm. The peak corresponding to p_0 would permit the probing of a larger thickness, but its small cross section normally prevents its use.

2.3. Cross section

^{6}Li-induced reactions generally have cross sections between 0.1 and 1 mb/sr. With a beam current of 10 nA of $^6Li^+$ and a detector solid angle of 10 msr, this cross section gives a count rate of about 0.1 count per second for quantities lying between 10^{17} and 10^{18} at/cm^2. With optimized conditions, it is possible to profile 10^{16} at/cm^2.

Some cross sections have been measured in the energy interval of interest. Fig. 5 shows the curves for ^{6}Li+^{12}C at 165°. They are typical of ^{6}Li-induced reactions. They present marked but rather smooth variations with energy, and there exist regions where these variations are minimum so that the analysis does not require complicated unfolding procedures.

In conclusion, we can see that ^{6}Li can be a useful beam for materials analysis. It can be used for conventional backscattering on heavy elements, and at the same time it can induce nuclear reactions useful for detecting and profiling light elements. Since the energy needed is only 6 MeV, suitable beams can be produced with small accelerators (as $^6Li^{++}$). Finally, it is worth mentioning that even in isotopic form, it is inexpensive as feedstock for the ion source.

3. Elastic recoil detection analysis

One unsatisfying aspect of ^{6}Li reactions comes from the cross sections: they are rather small when compared with Rutherford cross sections; they tend to vary in a seeming by arbitrary manner with angle and energy; and they have to be accurately known, which is not always the case. From that point of view some of the simplicity and beauty of Rutherford backscattering spectrometry is lost. One way to improve that is to look at the light nuclei recoiling after being hit by a heavier ion. This is the principle of the second technique of profiling light elements which we call "elastic recoil detection analysis". When a light nucleus elastically scatters a heavy incoming ion, it recoils with an energy given by

$$E_2 = E_1 \left[\frac{4M_1M_2}{(M_1+M_2)^2} \cos^2\theta \right] = kE_1 ,$$

where the symbols have the same significance as in fig. 3. If the collision takes place at depth x, the energy of the recoils coming out of the target will be

$$E_2''(x) = kE_1(0) - Fx .$$

The recoils of course come out only in the forward direction and an absorber will be necessary to stop the large flux of scattered incident ions so that upon reaching the detector the energy of recoils will be

$$E_2(x) = kE_1(0) - Fx - \Delta E_2 ,$$

where ΔE_2 is the energy loss in the absorber. It should be noted that k, F, and ΔE_2 depend on the type of recoiling nucleus. This method is discussed below from the points of view of selectivity, depth resolution, and sensitivity.

3.1. Selectivity

The selectivity is given by the variation in the kinematic factor k. k is small for M_1 very different

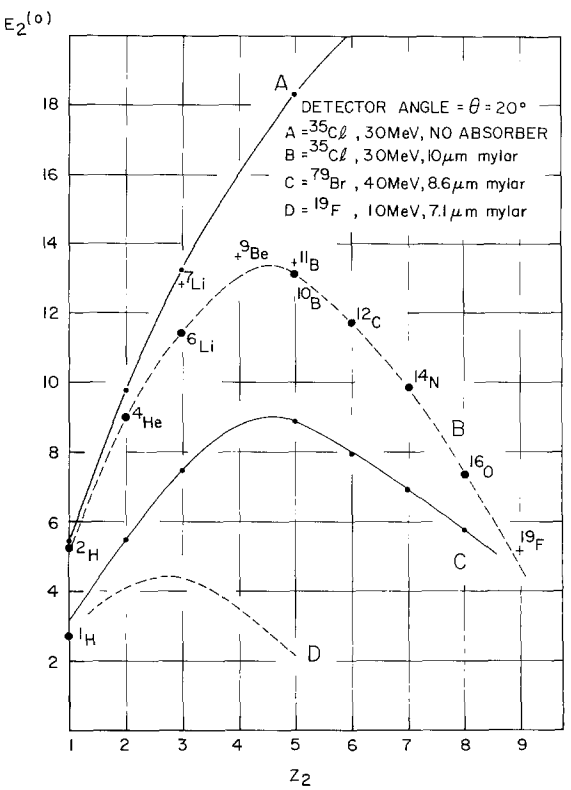

Fig. 6. Energy of the particles reaching the detector at 20° after being hit by various ion beams. The curves link recoils with an equal number of protons and neutrons. Curves A and B are for a 30 MeV ^{35}Cl ion beam. In curve B, a 10 μm mylar absorber was used to shield the detector from the scattered ^{35}Cl ions. All the specifically identified points belong to this curve.

from M_2 and is equal to $\cos^2\theta$ for $M_1 = M_2$. The best selection is obtained near 0° where $\cos\theta$ is equal to one. However, the necessity of using an absorber will modify drastically the energy of the recoils in the detector. This property is shown in fig. 6 for recoils ejected from the surface by various ion beams available at our machine. Since the absorber is just thick enough to stop the scattered incident ions, it is clear that recoils with mass, and therefore energy, close to that of the incident ions will lose most of their energy in the absorber. Accordingly the energy of the recoils will go through a maximum. The height and position of this maximum for a given incident ion beam depend on the angle and absorber thickness. We thus have a folding spectrometer. Possible ambiguities can however be lifted by a change in angle or foil thickness as exemplified in fig. 7. It is clear that ^{35}Cl at 30 MeV gives a wider range of outgoing energies and is a better choice from that point of view.

3.2. Depth resolution

The depth resolution depends on the type and energy of the incident beam, as can be seen from the definition of the depth factor given above. An increase in the mass of the incoming ion increases its specific energy loss but tends to decrease the kinematic factor so that the product $k(\mathrm{d}E/\mathrm{d}x)_1$ remains fairly constant at least for the lightest detected nuclei when the energy of the incoming beam is chosen so as to maximize $(\mathrm{d}E/\mathrm{d}x)_1$. Fig. 8 shows the depth resolution that can be obtained at a detection angle of 20° for different particles incident on an aluminium matrix. The energy resolution of the system depends on the detector (20 keV for protons to 100 keV for ^{19}F), the kinematic broadening, and the straggling in the mylar absorber, which we estimated from the Bohr formula[7]). Since with our machine ^{35}Cl represents the best overall choice, we have also estimated the depth resolution for a detection angle of 30°. It is interesting to note that the expected resolution is essentially the same for all elements (with the ex-

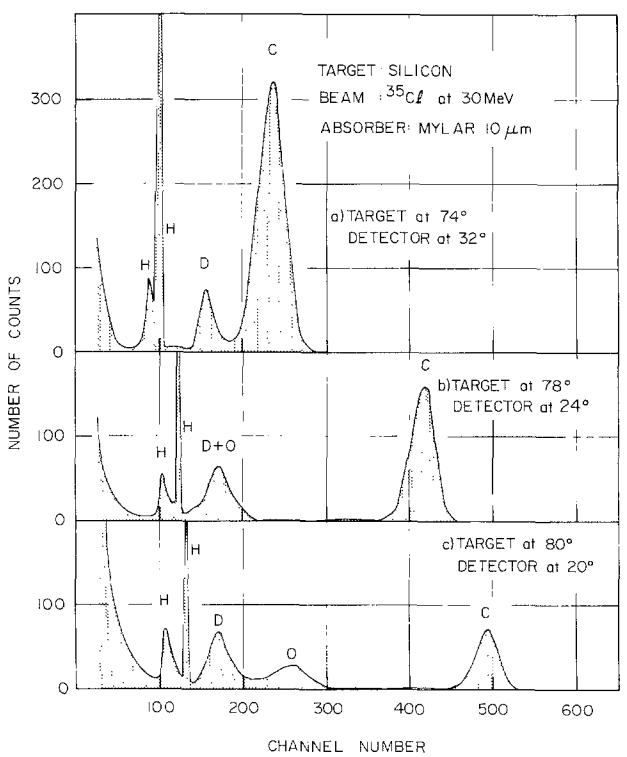

Fig. 7. Spectra of particles recoiling at various angles, from a silicon target containing small quantities ($\sim 10^{16}$ at/cm^2) of ^{1}H, ^{2}D, ^{12}C and ^{16}O. The incoming beam was ^{35}Cl at 30 MeV.

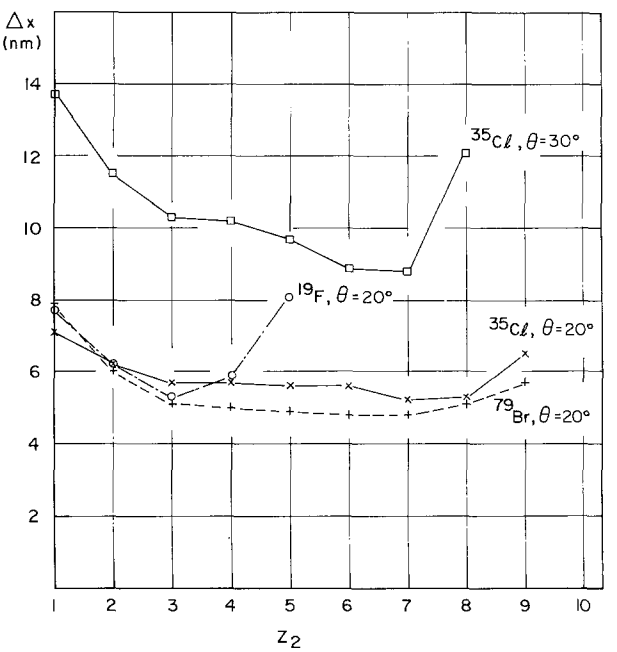

Fig. 8. Depth resolution near the surface for various elements present in an aluminium matrix at detection angles of 20° and 30°. The curves are for nuclei with an equal number of protons and neutrons, bombarded by ^{19}F at 10 MeV, ^{35}Cl at 30 MeV and ^{79}Br at 40 MeV. Mylar absorbers of 7.1 μm, 10 μm, and 8.6 μm respectively were used to shield the detector. The angular opening was 0.5° for ^{19}F and 0.25° in the other cases. The ^{1}H depth resolution for ^{35}Cl at 20° is estimated to be 12 nm.

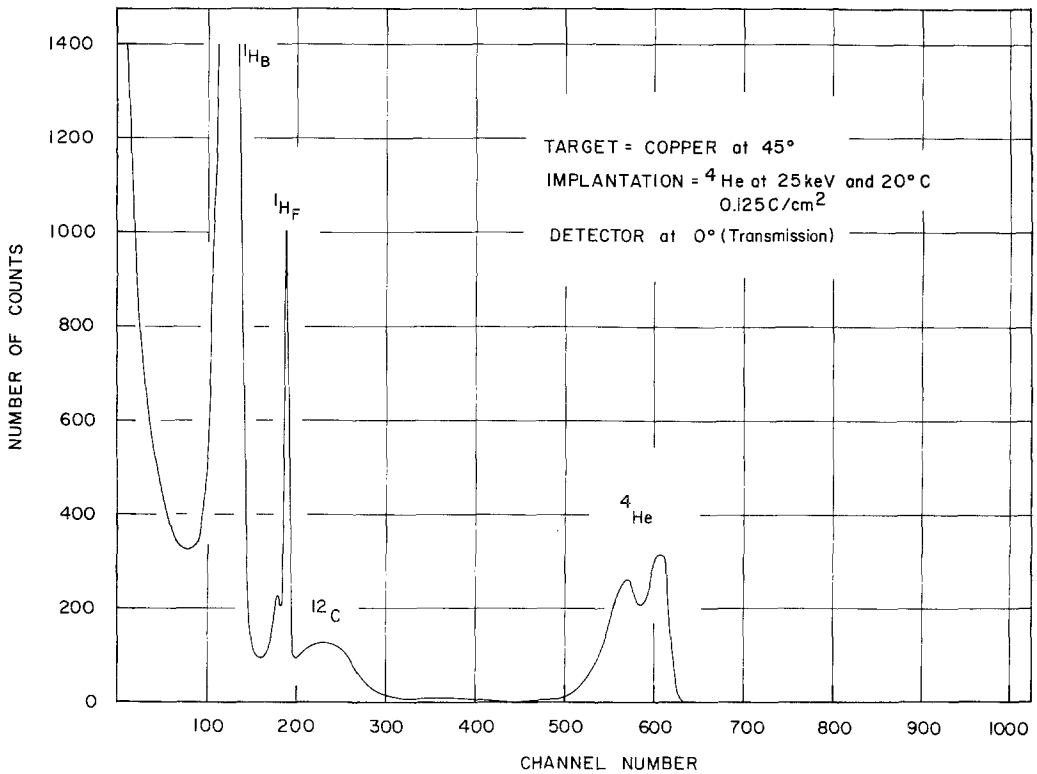

Fig. 9. Spectrum of the recoils from a copper target implanted with ^{4}He. The ^1H_F and ^1H_B peaks come from the presence of ^{1}H at the front and back of the thin copper target. The shape of the ^{4}He peak is characteristic of a high-dose implantation.

ception of ^{1}H). This comes from the fact that the increase in the depth factor coming from the kinematic factor k is nearly exactly compensated by the degradation in resolution from the straggling in the mylar absorber.

3.3. Cross section

With a 30 MeV ^{35}Cl beam, the energy in the center of mass system is well below the Coulomb barrier for any element so that the cross section can be calculated from the Rutherford formula. It gives roughly constant cross sections of 1 b/sr for recoils at 20° and 2 b/sr at 40°. Therefore quantities of 10^{16} at/cm^2 yield count rates of 0.1 count per second for solid angles of 1 msr and beam intensities of 1 particle-nA.

One interesting application is the detection of ^{4}He, which is somewhat difficult to perform by nuclear reactions. Fig. 9 shows the result of a profile measurement of helium implanted at 25 keV in copper. Here the target was thin, and the profile was obtained by transmission. The two peaks are characteristic of a high-dose implantation, and electron microscope studies indicate that they coincide with the formation of blisters[8]) (fig. 10). Calculations of the retained doses lead us to believe that the double peak is in fact due to a depletion of the profile curve coming from the release of helium accumulated in the blisters.

4. Conclusion

By virtue of its simplicity, its generality, its excellent depth resolution, and its sensitivity, the recoil analysis method is potentially more interesting than ^{6}Li-induced reactions, at least if one has access to the heavy-ion beams required. The probing depth will, however, generally be smaller than with ^{6}Li beams since the necessity to go to extreme forward angles requires a strong target tilt. The recoils analysis is particularly well adapted for the very light nuclei (such as ^{4}He) which are usually difficult to profile by other methods.

The authors are pleased to acknowledge the financial assistance of the National Research Council of Canada and of the Quebec Ministry of Education.

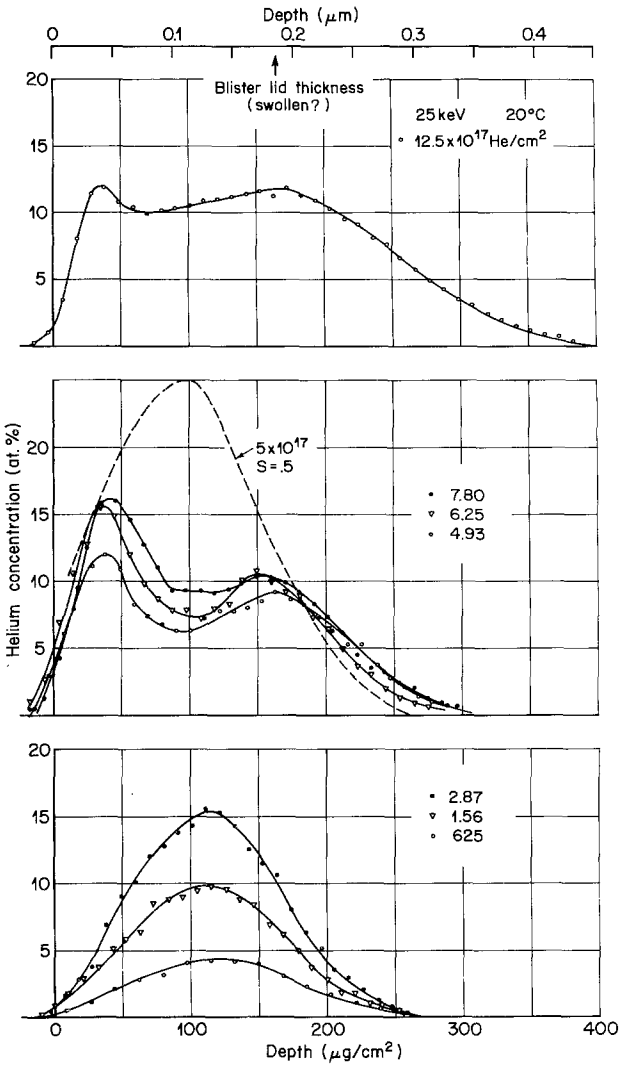

Fig. 10. Depth profiles of 25 keV ^{4}He ions implanted in copper films at room temperature at various doses. (Bottom) Low dose, $(0.625–2.87)\times10^{17}$ He/cm^2. (Middle) Higher dose, $(4.93–7.8)\times10^{17}$ He/cm^2. The dashed curve is the expected profile at 5×10^{17} He/cm^2 based on an assumed sputtering yield of 0.5 Cu atom/He ion. (Top) High dose, 12.5×10^{17} He/cm^2. No surface effect is detectable at low dose, but abundant blistering occurs at and above 4.93×10^{17} He/cm^2.

References

1) G. Amsel, J. P. Nadai, E. d'Artemare, D. David, E. Girard and J. Moulin, Nucl. Instr. and Meth. **92** (1971) 481; E. A. Wolicki, in *New uses of ion accelerators* (ed. J. F. Ziegler; Plenum Press, New York and London, 1975) p. 159.

2) J. L'Ecuyer, C. Brassard, C. Cardinal, L. Deschênes, Y. Jutras and J. P. Labrie, Nucl. Instr. and Meth. **140** (1977) 305.

3) J. L'Ecuyer, C. Brassard, C. Cardinal, J. Chabbal, L. Deschênes, J. P. Labrie, B. Terreault, J. G. Martel and R. St-Jacques, J. Appl. Phys. **47** (1976) 381.

4) C. Cardinal, C. Brassard, J. Chabbal, L. Deschênes, J. P. Labrie, J. L'Ecuyer and M. Leroux, Appl. Phys. Lett. **26** (1975) 543.

5) W. K. Chu, in *New uses of ion accelerators* (ed. J. F. Ziegler; Plenum Press, New York and London, 1975) p. 135.

6) L. C. Northcliffe and R. F. Schilling, Nucl. Data Tables **7** (1970) 233.

7) N. Bohr, Phil. Mag. **30** (1915) 581.

8) B. Terreault, J. G. Martel, R. G. St-Jacques, G. Veilleux, J. L'Ecuyer, C. Brassard, C. Cardinal, L. Deschênes and J. P. Labrie, to be published in J. Nucl. Mat.